Available online at www.sciencedirect.com
SCIENCE DIRECT®
Physica B 346–347 (2004) 421–427
PHYSICA B
www.elsevier.com/locate/physb

Pulsed magnetic fields as a probe of self-assembled semiconductor nanostructures

M. Hayne[a,*], J. Maes[a], S. Bersier[a], M. Henini[b], L. Müller-Kirsch[c], Robert Heitz[c], D. Bimberg[c], V.V. Moshchalkov[a]

[a] *Laboratorium voor Vaste-Stoffyscia en Magnetisme, Katholieke Universiteit Leuven, Celestjinenlaan 200D, Leuven B-3001, Belgium*
[b] *School of Physics and Astronomy, University of Nottingham, University Park, Nottingham NG7 2RD, UK*
[c] *Institut für Festkörperphysik, Technische Universität Berlin, Hardenbergstrasse 36, Berlin 10623, Germany*

Abstract

Pulsed magnetic fields are used to study a variety of self-assembled semiconductor nanostructures. We illustrate the power of the technique with two recent examples. In the first, we study confinement in InAs quantum dots on (1 0 0) and (3 1 1)B oriented GaAs substrates as a function of InAs coverage. We demonstrate that Stranski–Krastanow growth occurs for (1 0 0) substrates, but show that for (3 1 1)B substrates there is no such transition—rather the dots evolve from fluctuations in the wetting layer. In the second example, we investigate the Coulomb binding of 'free' electrons to holes confined to type-II GaSb/GaAs quantum dots. We find that at low laser power the electrons are repelled from the dots (by strain), but that by optical pumping the dots may be multiply charged, attracting the electrons, and more than doubling the binding energy.

PACS: 73.21.La; 78.55.Cr; 78.67.Hc

Keywords: Self-assembled quantum dots; Pulsed magnetic fields

1. Introduction

The magnetic length, $\ell_0 = \sqrt{\hbar/eB}$ is a few nanometers in magnetic fields, B, of the order of a few tens of tesla, making large magnetic fields a natural tool for the investigation of semiconductor and other nanostructures. For the last 5 years we have been using the pulsed field facility at the KU Leuven to study the confinement and excitonic properties of a wide variety of self-assembled semiconductor nanostructures (for a review of self-assembled quantum dots see Ref. [1]). Initial work was focused on InP self-assembled quantum dots (QDs) in $GaInP_2$ [2,3], but has recently expanded to include InAs QDs in GaAs [4,5], GaSb QDs in GaAs [6] and InAs quantum wires in InP [7].

Here, we illustrate the technique with two examples of recent magneto-photoluminescence experiments on self-assembled QDs. In the first we show how the confinement properties of the dots can be investigated using this technique. Specifically, we investigate the formation of InAs QDs, which confine both electrons and holes,

*Corresponding author. Tel.: +32-16-327202; fax: +32-16-327983.
E-mail address: manus.hayne@fys.kuleuven.ac.be (M. Hayne).

0921-4526/$ - see front matter © 2004 Elsevier B.V. All rights reserved.
doi:10.1016/j.physb.2004.01.119

on (1 0 0) and (3 1 1)B oriented substrates [4]. In the second example we study excitonic effects, namely the Coulomb binding of electrons to holes that are confined to type-II GaSb/GaAs QDs [6].

2. Photoluminescence experiments in pulsed magnetic fields

Photoluminescence (PL) experiments are conducted in 50 T pulsed field coils developed in the laboratory [8] in combination with a 5 kV, 600 kJ capacitor bank [9], though a 70 T user coil connected to a 10 kV, 500 kJ capacitor bank has recently become available [10]. Both ^{4}He bath and flow cryostats are used for PL experiments making temperatures between 1.5 and 200 K accessible. A 11.5 T DC magnet with variable temperature insert (1.5–300 K) is also configured for optical access. Samples can be excited at wavelengths varying from UV (275.4 nm) to green (532 nm) using Ar^+ or solid-state lasers, providing typically $\sim$1 W cm^{-2} at the sample surface. The laser light is transmitted to the sample via a single 200-μm-core fibre, and is collected by a single large (550 μm) core fibre or a bundle of smaller (200 μm) core fibres. The PL is analysed in a 0.275 m spectrometer with an intensified CCD detector or a 0.3 m spectrometer with an InGaAs diode array, providing sensitivity between 400 and 1700 nm. For both detection systems several spectra may be obtained during each 22 ms field pulse. Typical photon integration times vary between 0.5 and 2 ms, depending on the sample under investigation and the timing of the exposure with respect to the field pulse. The field variation for any particular spectrum is rarely more than $\pm$ 3%, and for data taken at the peak of the pulse it can be one or two orders of magnitude smaller (Fig. 1). The equipment is configured such that either of the lasers and spectrometer/detector systems may be used in combination with any of the magnets/cryostats. Further details may be found in Refs. [2–7,9]. All experiments discussed herein were conducted at 4.2 K with the field perpendicular to the plane of the samples. The detector was the InGaAs array. Unless otherwise stated, the laser power density at the sample was $\sim$1 W cm^{-2}.

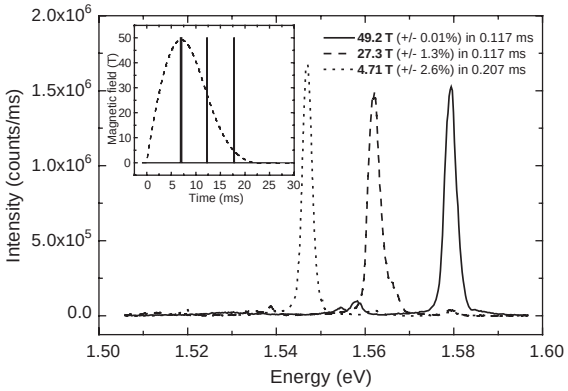

Fig. 1. Typical photoluminescence data acquisition in pulsed fields, in this case for a single GaAs quantum well. The main part of the figure shows three spectra taken at 49.2, 27.3 and 4.71 T in a single shot. The inset shows the corresponding field profile and the timing of the three exposures with respect to the field pulse.

3. InAs quantum dot formation on (1 0 0) and (3 1 1)B GaAs substrates

The basic idea behind the use of pulsed magnetic fields in the investigation of semiconductor nanostructures is that when a sufficiently strong magnetic field is applied, the magnetic confinement can compete with, and even overcome, the spatial confinement. In terms of length scales this happens when the magnetic length is smaller than the exciton Bohr radius a_B in the plane perpendicular to the applied field [3]. If the exciton wavefunction (confinement) is strongly anisotropic in the plane, it is the smallest length scale that determines the transition to the high-field regime [5]. In this limit, the PL energy increases linearly with magnetic field, parallel with the lowest Landau level. Below the high-field limit, where the spatial confinement still dominates, the effect of an applied field is much smaller, and the diamagnetic shift is given by $\Delta E = (e^2 a_B^2/8\mu)B^2$, where μ is the reduced exciton mass. In general, it is clear that the stronger the spatial confinement of the carriers, the smaller the diamagnetic shift.

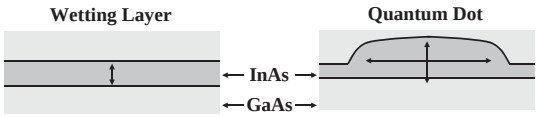

Fig. 2. Schematic representation of the difference in confinement between wetting layer (WL) and quantum dot (QD). The WL gives strong vertical confinement and no lateral confinement, whereas the dot does impose lateral confinement, but with vertical confinement that is weaker than that of the WL.

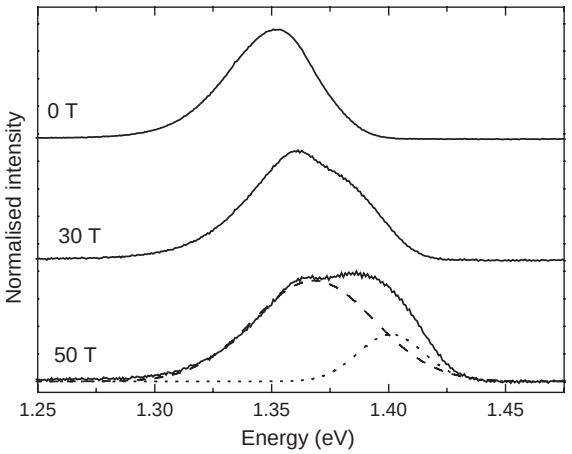

Fig. 3. Low-temperature spectra for 1.5 ML of InAs on a (1 0 0) GaAs substrate at different magnetic fields. As the field is increased the line develops a high-energy shoulder, such that the spectrum at 50 T can be resolved into broad (dashed line) and narrow (dotted line) components.

We illustrate how this may be exploited in the study of self-assembled QDs with the results obtained for InAs dots grown on (1 0 0) and (3 1 1)B GaAs substrates at the University of Nottingham [4,11,12]. The idea behind the experiment is illustrated in Fig. 2, where we schematically show the confinement in the growth direction and the (x, y) plane of the sample from a wetting layer (WL) and from a QD. It can be seen that for the WL there is no confinement in the plane, but strong confinement in the growth direction. On the other hand, the QD has weaker vertical but some lateral (x, y) confinement. Thus the application of a magnetic field in the growth direction should allow us to distinguish between WL and QD, and thus investigate the formation of the QDs.

Fig. 3 shows the spectra of a sample with 1.5 monolayers (ML) of InAs on (1 0 0) GaAs at 0, 30 and 50 T. The zero-field spectrum shows a single broad Gaussian peak (51 meV line width), characteristic of an ensemble of dots. Such a spectrum may lead us to conclude that the dots are fully formed [11]. However, as the magnetic field is increased to 30 and then to 50 T, a high-energy shoulder, from a second, much narrower peak (line width 28 meV), becomes evident. This peak is due to recombination from the WL, and demonstrates that for this coverage, both QDs and WL coexist in the sample, i.e. that the QDs are not fully formed. An examination of Fig. 2 elucidates the role of the magnetic field in revealing the WL PL. At zero and low fields the total confinement (and thus PL) energy of the QD and WL coincide. As the field is applied additional lateral confinement is imposed on carriers in the WL, increasing the PL energy. Since lateral confinement already exists for carriers in the QDs, the magnetic field has less effect than it does for the WL, and the peaks separate. Indeed, it is clear that at the point at which the field confinement overcomes the lateral spatial confinement of the QDs, the difference in PL energies for WL and QD originates in the strong vertical confinement of the WL.

Further insight into QD formation can be gained by studying the size of the diamagnetic shift between 0 and 50 T as a function of InAs coverage, as shown in Fig. 4 for dots grown on (1 0 0) and (3 1 1)B substrates. For (1 0 0) sub-

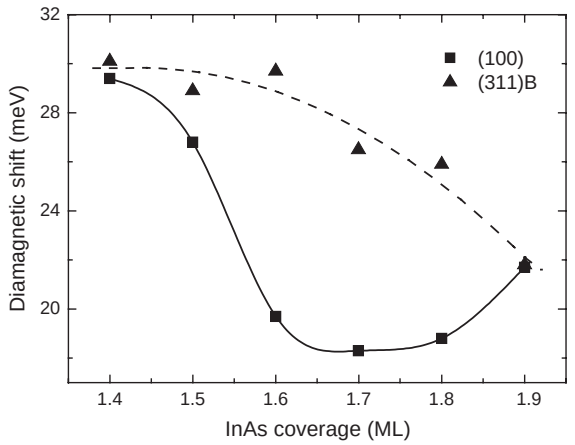

Fig. 4. Dependence of the diamagnetic shift of the PL between 0 and 50 T as a function of InAs layer coverage. The lines are guides to the eye.

strates there is a clear drop in the size of the diamagnetic shift between 1.5 and 1.6 ML, indicative of a sudden increase of the lateral confinement. We attribute this to the Stranski–Krastanow growth transition, signalling the full formation of the dots across the sample. This is consistent with the appearance of the transition determined during the growth of the samples from reflection high-energy electron diffraction (RHEED) to be 1.7 ML [12]. As further material is deposited we observe a slight increase in the diamagnetic shift, due to the formation of larger (and more relaxed) dots.

In contrast, for dots grown on (3 1 1)B substrates, there is no such transition, but a gradual decrease in the diamagnetic shift. We interpret this as a smooth evolution of the dots from fluctuations in the thickness of the WL, rather than true Stranski–Krastanow growth. The difference between the two substrate orientations is thought to arise from reduced atomic diffusion rates on the atomically rough (3 1 1)B tilted substrate [4,11,13].

4. Coulomb binding of electrons to holes in type-II GaSb dots

In the previous section we illustrated how a large magnetic field can be used to probe the confinement in type-I quantum dots, i.e. dots which confine both electrons and holes. It is also possible to grow dots in which only one type of carrier is confined by the band offsets, i.e. either the electrons or the holes, but not both. This is illustrated in Fig. 5, which depicts type-I and type-II confinement. GaSb/GaAs QDs are a primary example of type-II QDs in which the holes are strongly confined [14], but the electrons are expelled (Fig. 5(b)). In such a situation it is only the Coulomb interaction between the 'free' electron and the confined hole that keeps the electron in the proximity of the dot, and it is this on which we now focus our attention.

Fig. 6 shows a typical zero-field spectrum for a GaSb/GaAs QD sample grown at the Technische Universität Berlin [15], taken with an incident laser power of 30 W cm^{-2}. Three spectral regions may be identified. The broad low-intensity peak at 1.15 eV arises from the QDs, the intense broad peak at 1.38 eV is attributed to the WL, and the group of lines around 1.5 eV arise from the GaAs matrix around the dots.

We first discuss the field dependence of the WL peak, which is shown in Fig. 7(a). As mentioned in Section 3 above, the diamagnetic shift is parabolic in B at low fields and linear in B at high fields. We can construct a single function that describes the behaviour in both limits by requiring that it and its derivative are continuous in the crossover between the two regimes. Doing so we obtain the following expression for the PL energy E as a function of B [3]:

$$E = E_0 + \frac{e^2 a_B^2}{8\mu} B^2, \quad \text{for } B < \frac{2\hbar}{e a_B^2}, \tag{1a}$$

$$E = E_0 - \frac{\hbar^2}{2\mu a_B^2} + \frac{\hbar e B}{2\mu}, \quad \text{for } B > \frac{2\hbar}{e a_B^2}. \tag{1b}$$

This analysis is based on an excitonic model of QDs, and is therefore applicable to structures with all dimensionalities. The second term on the right-hand side of Eq. (1b) is the exciton (hydrogenic)

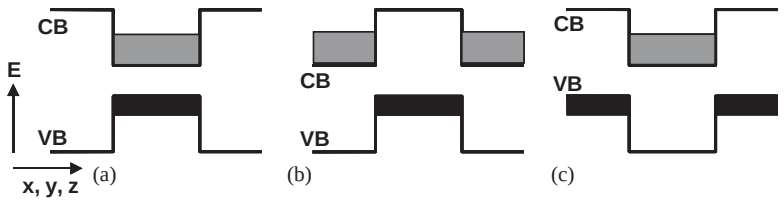

Fig. 5. Schematic representation of the difference in (a) type-I and (b), (c) type-II confinement. The vertical axis is energy, and the horizontal axis represents any spatial direction. In type-I confinement (a), as is the case for InAs quantum dots, the band offsets localise both electrons and holes. In type-II confinement, either the holes are located in the dots and the electrons are outside (b), as is the case for GaSb quantum dots, or vice versa (c). It is interesting to note that by engineering the strain, e.g. by stacking the dots, band offsets may be altered to change the confinement from type-I to type-II (see, for example, Ref. [5], and references therein).

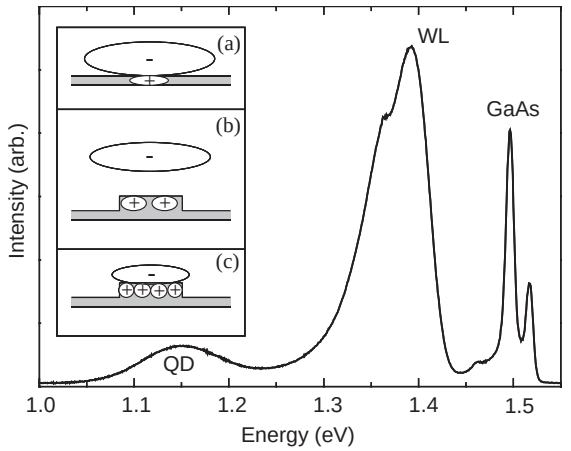

Fig. 6. Low-temperature zero-field spectrum for a GaSb/GaAs QD sample at a laser power of 30 W cm^{-2}. The shoulder on the low-energy side of the WL peak is an artefact due to a step-like increase in the response of the InGaAs array. The inset schematically shows the size and displacement of the electron from the GaSb (shaded region) for (a) WL, (b) QD under low intensity illumination and (c) QD under high intensity illumination. The number of holes in (b) and (c) are intended to signify a greater or lesser occupation, rather than actual occupancies.

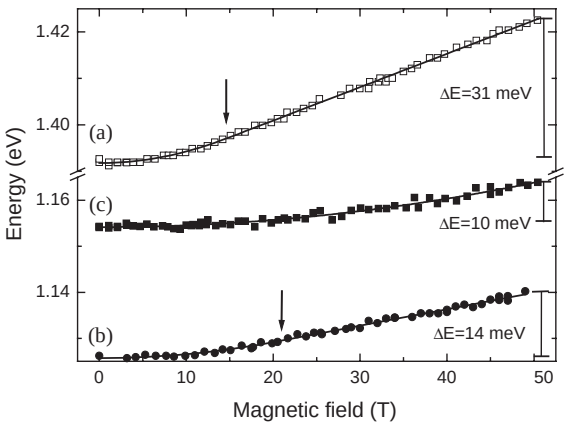

Fig. 7. Peak position of (a) WL PL at 30 W cm^{-2}, (b) QD PL at 0.5 W cm^{-2} and (c) QD PL at 30 W cm^{-2}. The arrows indicate the field at which the transition from parabolic to linear field dependence occurs.

binding energy, and the third term is the energy of the lowest Landau level. It is important to stress that the whole function, i.e. Eqs. (1a) and (1b), is readily fitted to the same data in one operation, and that three physically meaningful fitting parameters are obtained, namely, a_B, μ and E_0, the PL energy at zero field. In this model the cross-over between the high- and low-field regimes occurs at $\ell_0 = a_B/\sqrt{2}$.

In applying this to GaSb/GaAs QDs we should bear in mind that the electron effective mass is about 10 times smaller than the hole effective mass for both GaAs and for GaSb. Furthermore, since it is the electron that is free and the hole which is confined, we can be confident that the properties we measure are essentially those of the electron, and we can expect a hydrogenic model of the system to work well. Indeed, for the WL we obtain $\mu = 0.081\ m_0$, where m_0 is the free electron mass, and $a_B = 9.5$ nm, which are closer to the values for GaAs (0.067 m_0 and 10 nm, respectively), than for GaSb (0.039 m_0 and 21 nm, respectively). Substituting these into $a_B = a_B^0\varepsilon/(\mu/m_0)$ where $a_B^0 = 0.529$ Å is the Bohr radius of the hydrogen atom, and ε is the relative dielectric constant, gives an ε of 14.5, which is the arithmetic mean of the values for GaSb and GaAs (15.7 and 13.2, respectively). Thus the data are indeed consistent with holes confined to the GaSb WL, and electrons bound by the Coulomb interaction to the GaAs matrix above or below the WL, as expected. This is shown schematically in panel (a) of the inset to Fig. 6. Expressing the electron–hole interaction in terms of the binding energy, $E_B = \hbar^2/2\mu a_B^2$ defined by Eq. (1b), we obtain a value of 5.2 meV. It should be noted that the field dependence of the WL peak is invariant with laser power.

The energy of the QD peak as a function of magnetic field at an incident laser power of 0.5 W cm^{-2} is shown in Fig. 7(b). It can be seen that the size of the diamagnetic shift has been reduced by almost exactly a factor of two, and that the field at which the high-field limit is reached, as shown by the arrow, has increased slightly compared to the WL data in Fig. 7(a). The former is readily explained by a doubling of μ to 0.16 m_0, while the latter indicates a small reduction in the Bohr radius. The interesting point is that since $a_B = a_B^0\varepsilon/(\mu/m_0)$, doubling the exciton mass should halve a_B, and so increase the field at which the high-field limit is reached

by a factor of four. This is clearly not the case. The Bohr radius is therefore much *larger* than we would expect, indicating a reduction of the Coulomb interaction between the electron and the hole, due to their spatial separation. In fact, 8 band **k**.**p** calculations have shown that this is the result of electron repulsion by strain-induced warping of the conduction band in the GaAs matrix surrounding the dot [6]. Again, we quantify the electron–hole interaction in terms of the binding energy, obtaining a value of 3.7 meV for these data.

In contrast to the WL PL, we find that the field dependence of the QD PL varies with laser power. This can be seen from Fig. 7(c), where we show data for 30 W cm^{-2}, the same laser power density as was used for the WL data in Fig. 7(a). Two crucial differences are seen compared with the low-power QD data in Fig. 7(b). Firstly, the zero field peak position has increased by some 28 meV, which is a result of charging of the dots with holes by optical pumping [16]. Secondly, the data remain parabolic in B to the highest fields, and as a consequence, the size of the diamagnetic shift is only 10 meV. Thus, we now have a situation in which the Bohr radius is considerably reduced. With a μ that is the same as at low power, we find a transition to the high-field regime of 47 T, and a corresponding a_B of 5.3 nm. Since the slope of the data in Fig. 7(c) can only increase, not decrease, at higher fields, these values of μ and a_B are both *upper limits*. Expressing this in terms of the binding energy, we obtain 8.4 meV, which is more than double than what it was at low power, and is a *lower limit*. These data therefore demonstrate that compared to the situation at low laser power, the electron responsible for the PL is tightly bound to the dot, and as a result has a significantly reduced Bohr radius. We attribute this to an enhanced Coulomb interaction between a single closely bound 'core' electron, and a dot that is multiply charged with holes by optical pumping. This is illustrated in the inset to Fig. 6 panel (b) of which shows the case where the dot is weakly charged. Strain pushes the electron away from the dot [6], and the weakened Coulomb interaction increases the lateral Bohr radius. At high power the strong Coulomb attraction from the multiply charged dot is able to (partially) overcome the strain-induced repulsion, and the electron becomes tightly bound, increasing the binding energy and reducing a_B (inset of Fig. 6, panel (c)). Finally, we remember that the diamagnetic shift of the WL PL is found to be independent of laser power. This is simply because the holes are free to drift apart in the plane of the sample, excluding the multiple-charging effects observed for the dots.

5. Conclusions

Magneto-photoluminescence in pulsed fields can make a unique contribution to the study of self-assembled semiconductor nanostructures, giving new insight into their fundamental properties, and information that can be exploited in the design of novel devices. In particular, this has been demonstrated with two examples of recent experiments on quite different systems. In the first, an investigation of InAs quantum dots revealed the differences in dot formation on (1 0 0) and (3 1 1)B oriented substrates. In the second we studied the Coulomb interaction between 'free' electrons and holes confined to GaSb/GaAs quantum dots. We found that at low laser power electrons are more weakly bound to holes that are confined to the dots than to those in the wetting layer. When the laser power is increased, Coulomb charging of the dots reverses this situation.

We fully expect that high-field magneto-photoluminescence will continue to reveal new physical phenomena in an increasingly wide variety of semiconductor nanostructures in the future.

Acknowledgements

This work is supported by the FWO-Vlaanderen, the Flemish GOA and the Belgian IUAP programmes, the VIS 00/001 project of the KU Leuven and the NANOMAT project of the Growth Programme of the EC, contract number G5RD-CT-2001-00545.

References

[1] D. Bimberg, M. Grundmann, N.N. Ledentsov, Quantum Dot Heterostructures, Wiley, Chichester, 1999.

[2] R. Provoost, M. Hayne, V.V. Moshchalkov, M.K. Zundel, K. Eberl, Appl. Phys. Lett. 75 (1999) 799;
M. Hayne, J. Maes, V.V. Moshchalkov, Y.M. Manz, O.G. Schmidt, K. Eberl, Appl. Phys. Lett. 79 (2001) 45.

[3] M. Hayne, R. Provoost, M.K. Zundel, Y.M. Manz, K. Eberl, V.V. Moshchalkov, Phys. Rev. B 62 (2000) 10324.

[4] J. Maes, M. Hayne, V.V. Moshchalkov, A. Patanè, M. Henini, L. Eaves, P.C. Main, Appl. Phys. Lett. 81 (2002) 1480.

[5] J. Maes, M. Hayne, M. Henini, F. Pulizzi, A. Patanè, L. Eaves, V.V. Moshchalkov, Magneto-photoluminescence of stacked self-assembled InAs/GaAs quantum dots, these Proceedings (RHMF 2003), Physica B 346–347 (2004).

[6] M. Hayne, J. Maes, S. Bersier, V.V. Moshchalkov, A. Schliwa, L. Müller-Kirsch, C. Kapteyn, R. Heitz, D. Bimberg, Appl. Phys. Lett. 82 (2003) 4335.

[7] J. Maes, M. Hayne, L. González, D. Fuster, J.M. Garcia, V.V. Moshchalkov, Physica E 21 (2-4) (2004) 261.

[8] L. Van Bockstal, G. Heremans, F. Herlach, Meas. Sci. Technol. 2 (1991) 1159;
L. Li, F. Herlach, Meas. Sci. Technol. 6 (1995) 1035.

[9] J. Vanacken, Physica B 294–295 (2001) 591.

[10] A. Lagutin, K. Rosseel, F. Herlach, Y.B. Bruynseraede, Durable 70 T Pulsed Magnets, Physica B, this conference.

[11] A. Lagutin, F. Herlach, J. Vanacken, Y. Bruynseraede, Meas. Sci. Technol. 14 (2003) 2144.

[12] S. Sanguinetti, G. Chiantoni, E. Grilli, M. Guzzi, M. Henini, A. Polimeni, A. Patanè, L. Eaves, P.C. Main, Europhys. Lett. 47 (1999) 701.

[13] P. Moriarty, Y.-R. Ma, A.W. Dunn, P.H. Beton, M. Henini, C. McGinley, E. McLoughlin, A.A. Cafolla, G. Hughes, S. Downes, D. Teehan, B. Murphy, Phys. Rev. B 55 (1997) 15397.

[14] M. Geller, C. Kapteyn, L. Müller-Kirsch, R. Heitz, D. Bimberg, Appl. Phys. Lett. 82 (2003) 2706.

[15] L. Müller-Kirsch, R. Heitz, U.W. Pohl, D. Bimberg, I. Häusler, H. Kirmse, W. Neumann, Appl. Phys. Lett. 79 (2001) 1027.

[16] L. Müller-Kirsch, R. Heitz, A. Schliwa, D. Bimberg, H. Kirmse, W. Meumann, Appl. Phys. Lett. 78 (2001) 1418.